On the temperature effects in QCD axion mass mixing

Hai-Jun Li

Key Laboratory of Theoretical Physics, Institute of Theoretical Physics, Chinese Academy of Sciences, Beijing 100190, China

E-mail: lihaijun@itp.ac.cn

ABSTRACT: In this work, we extend the QCD axion mass mixing in the early Universe and investigate the temperature effects in the mixing. We explore the scenario where two $Z_\mathcal{N}$ QCD axions undergo mass mixing during the QCD phase transition, yielding three distinct mixing scenarios: mixing I, II, and III. These scenarios are realized through fine-tuning of the axion decay constants, the temperature parameters, as well as the value of $\mathcal{N}$. We conduct a thorough analysis of the level crossing phenomena in these three mixing scenarios, detailing the conditions under which they occur. Notably, in the mixing I and II, the level crossing precedes the critical temperature of the QCD phase transition (T_{QCD}), with minimal non-essential discrepancies in the cosmological evolution of the mass eigenvalues at T_{QCD}. In contrast, the mixing III exhibits a unique double level crossings, occurring both before and at T_{QCD}. Despite superficial similarities in axion evolution between the mixing II and III, we uncover fundamental differences between them. Additionally, we briefly address the transition in energy density between the two axions within our mixing scenarios. This work contributes to a deeper understanding of the role of the QCD axion in the early Universe and its potential implications for dark matter.

Contents

1 Introduction

The QCD axion holds the remarkable potential to address two fundamental issues simultaneously: the strong CP problem and the mystery of dark matter (DM). It was originally proposed by the Peccei-Quinn (PQ) mechanism [1, 2] with a spontaneously broken global $U(1)_{\mathrm{PQ}}$ symmetry to solve the strong CP problem in the Standard Model (SM) [3–8]. It acquires a minuscule mass from the QCD non-perturbative effects [9, 10]. When the QCD instanton generates the axion potential, the axion can stabilize at the CP conservation minimum, which dynamically solves the strong CP problem. See ref. [11] for a review.

On the other hand, the QCD axion is attractive candidate for the cold DM that non-thermally produced through the misalignment mechanism [12–14]. The oscillation of coherent axion state in the potential in the early Universe can contribute to the overall DM. The equation of motion (EOM) for this state is that of a damped harmonic oscillator, in which the friction term is proportional to the Hubble parameter $H(T)$ and the spring constant is proportional to the axion mass $m_a(T)$. As the temperature decreases, the QCD axion gains a non-zero mass during the QCD phase transition and begins to oscillate when $m_a(T)$ is comparable to $H(T)$, the system thus changes from an overdamped to an underdamped oscillator and the oscillation explains the observed cold DM abundance. See also refs. [15–17] for recent reviews. By assuming the $\sim \mathcal{O}(1)$ initial misalignment angle, this mechanism gives the upper limit on the classical QCD axion window $f_a \lesssim 10^{11} - 10^{12}\,\mathrm{GeV}$, where f_a is the axion decay constant. While the lower limit $f_a \gtrsim 10^9\,\mathrm{GeV}$ is given by the SN 1987A [18–20] and the neutron star cooling [21–23].

In recent years, there have been several attempts to broaden the above classical QCD axion window, one of which is the lighter-than-usual axion model, the $Z_{\mathcal{N}}$ QCD axion

[24, 25]. In this scenario, the $\mathcal{N}$ mirror worlds that are nonlinearly realized by the axion field under a discrete $Z_{\mathcal{N}}$ symmetry can coexist in Nature. The zero-temperature $Z_{\mathcal{N}}$ axion mass is exponentially suppressed at the QCD phase transition critical temperature due to the suppressed non-perturbative effects on the axion potential. The $Z_{\mathcal{N}}$ axion can also simultaneously solve the strong CP problem and account for the DM. In order to solve the strong CP problem, here $\mathcal{N}$ should be an odd number and greater than or equal to 3. In addition, this lighter QCD axion can account for the cold DM through the trapped+kinetic misalignment mechanism [26, 27].

The Universe with a large number of these axions, the QCD axions or axionlike particles (ALPs), is called the axiverse [28–30]. In the axiverse, it is natural to take into account the cosmological evolution of the multiple axions. In recent years the mass mixing in the multiple axions model [31] has attracted extensive attention. If considering the non-zero mass mixing between two axions, the nontrivial cosmological evolution process of the mass eigenvalues called the level crossing can take place during the QCD phase transition, such as the mixing between the QCD axion and ALP [32], between the QCD axion and sterile axion [33], and between the $Z_{\mathcal{N}}$ axion and ALP [34], etc. In general, the level crossing can occur before the QCD phase transition critical temperature T_{QCD}. But this is not always the case, as pointed out in ref. [34], there may still be a second level crossing at T_{QCD} in the mixing with a $Z_{\mathcal{N}}$ axion, which is called the double level crossings. The level crossing can lead to the adiabatic transition of the axion energy density, which is similar to the MSW effect [35–37] in the neutrino oscillations. It also has some intriguing cosmological implications, including the modification of axion relic density and isocurvature perturbations [38–41], the formation of domain walls [42], the effects on gravitational waves and primordial black holes [43–45], and the composition of dark energy [46, 47], etc.

So far, above axion mass mixing can be summarized as a mixing between an axion possessing a temperature-dependent mass and one with a constant mass, but what emerges if considering two axions, both of which exhibit the temperature-dependent masses? In ref. [48], they recently investigated this mixing case with two QCD axions, one canonical QCD axion and one $Z_{\mathcal{N}}$ axion, showing a novel level crossing in the mass mixing.

In this work, we extend this QCD axion mass mixing and investigate the temperature effects in the mixing. We consider the mass mixing between two $Z_{\mathcal{N}}$ axions during the QCD phase transition, resulting in three mixing scenarios, the mixing I, II, and III. This can be accomplished by fine-tuning the model parameters. The level crossing in these three mixing scenarios and the conditions for them to occur are investigated in detail. In the mixing I and II, the level crossing can take place before T_{QCD}, while the cosmological evolution of the mass eigenvalues at T_{QCD} has a minor non-essential difference. In the mixing III, we find that the double level crossings can take place before and at T_{QCD}, respectively. Although the axion evolution in the mixing II and III appears similar, they have fundamental differences. Finally, we briefly discuss the axion energy density transition in the mixing. Our mixing scenarios may also have some intriguing cosmological implications.

The rest of this paper is structured as follows. In section 2, we briefly review the QCD axion. In section 3, we investigate the extended QCD axion mass mixing, focusing on the three mixing scenarios. Finally, the conclusion is given in section 4.

2 Brief review on QCD axion

In this section, we briefly review the QCD axion. We first introduce the canonical QCD axion. The canonical QCD axion effective potential from the QCD non-perturbative effects is given by

$$V_{\text{QCD}}(\phi) = m_a^2(T) f_a^2 \left[1 - \cos\left(\frac{\phi}{f_a} \right) \right], \tag{2.1}$$

where ϕ is the axion field, f_a is the axion decay constant, and $\theta = \phi/f_a$ is the axion angle. The $m_a(T)$ is the temperature-dependent QCD axion mass

$$m_a(T) = \begin{cases} \dfrac{m_\pi f_\pi}{f_a} \dfrac{\sqrt{z}}{1+z}, & T \leq T_{\text{QCD}} \\[2ex] \dfrac{m_\pi f_\pi}{f_a} \dfrac{\sqrt{z}}{1+z} \left(\dfrac{T}{T_{\text{QCD}}} \right)^{-b}, & T > T_{\text{QCD}} \end{cases} \tag{2.2}$$

where $T_{\text{QCD}} \simeq 150\,\text{MeV}$ is the critical temperature of the QCD phase transition, m_π and f_π are the mass and decay constant of the pion, respectively, $z \equiv m_u/m_d \simeq 0.48$ is the ratio of the up to down quark masses, and $b \simeq 4.08$ is an index taken from the dilute instanton gas approximation [49]. The first term in eq. (2.2) corresponds to the zero-temperature QCD axion mass $m_{a,0}^{\text{QCD}}$. The QCD axion can account for the DM through the misalignment mechanism. As the cosmic temperature decreases, the axion starts to oscillate when its mass $m_a(T)$ becomes comparable to the Hubble parameter $H(T)$. If considering the pre-inflationary scenario in which the PQ symmetry is spontaneously broken during inflation, the current QCD axion DM abundance can be described by

$$\Omega_a h^2 \simeq 0.14 \left(\frac{g_{*s}(T_0)}{3.94} \right) \left(\frac{g_*(T_{\text{osc}})}{61.75} \right)^{-0.42} \left(\frac{f_a}{10^{12}\,\text{GeV}} \right)^{1.16} \langle \theta_i^2 f(\theta_i) \rangle, \tag{2.3}$$

where $h \simeq 0.68$ is the reduced Hubble constant, T_0 is the current cosmic microwave background (CMB) temperature, T_{osc} is the axion oscillation temperature, and $f(\theta_i)$ is the anharmonicity factor [50, 51]. In order to explain the observed cold DM abundance, $\Omega_{\text{DM}} h^2 \simeq 0.12$ [52], we have the $\sim \mathcal{O}(1)$ initial misalignment angle

$$\theta_i \simeq 0.87 \left(\frac{g_{*s}(T_0)}{3.94} \right)^{-1/2} \left(\frac{g_*(T_{\text{osc}})}{61.75} \right)^{0.21} \left(\frac{f_a}{10^{12}\,\text{GeV}} \right)^{-0.58}. \tag{2.4}$$

In the $Z_{\mathcal{N}}$ axion scenario [24–26], the $\mathcal{N}$ copies of the SM worlds that are nonlinearly realized by the axion field under a $Z_{\mathcal{N}}$ symmetry ($0 \leqslant k \leqslant \mathcal{N} - 1$)

$$\text{SM}_k \to \text{SM}_{k+1}, \tag{2.5}$$

$$\phi \to \phi + \frac{2\pi k}{\mathcal{N}} f_a, \tag{2.6}$$

can coexist with the same coupling strengths as that in the SM

$$\mathcal{L} = \sum_{k=0}^{\mathcal{N}-1} \left[\mathcal{L}_{\text{SM}_k} + \frac{\alpha_s}{8\pi} \left(\frac{\phi}{f_a} + \frac{2\pi k}{\mathcal{N}} \right) G_k \widetilde{G}_k \right] + \cdots, \tag{2.7}$$
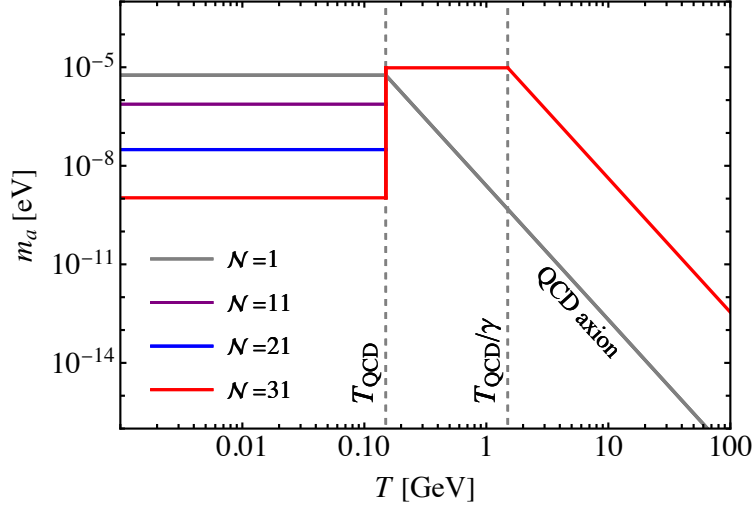
Figure 1. The temperature-dependent $Z_{\mathcal{N}}$ axion mass $m_a(T)$ as functions of the cosmic temperature T. The different colored lines represent the different values of $\mathcal{N}$, which are degenerated into the red line at $T \geq T_{\mathrm{QCD}}$. The vertical gray lines represent the temperatures T_{QCD} and T_{QCD}/γ, respectively. Notice also that the case $\mathcal{N} = 1$ (gray solid line) corresponds to the canonical QCD axion [eq. (2.2)]. Here we set $f_a = 10^{12}\,\mathrm{GeV}$ and $\gamma = 0.1$.

where $\mathcal{L}_{\mathrm{SM}_k}$ corresponds to the copies of the SM Lagrangian, $G_k \widetilde{G}_k$ is the topological term, and α_s is the strong fine structure constant. The $Z_{\mathcal{N}}$ axion has a nontrivial temperature-dependent potential. In the large $\mathcal{N}$ limit, the total axion potential can be given in all generality by

$$V_{\mathcal{N}}(\phi) \simeq -\frac{m_a^2(T) f_a^2}{\mathcal{N}^2} \cos\left(\mathcal{N}\frac{\phi}{f_a}\right) , \tag{2.8}$$

and the temperature-dependent $Z_{\mathcal{N}}$ axion mass can be described by

$$m_a(T) \simeq \begin{cases} \dfrac{m_\pi f_\pi}{\sqrt[4]{\pi} f_a} \sqrt[4]{\dfrac{1-z}{1+z}} \mathcal{N}^{3/4} z^{\mathcal{N}/2} , & T \leq T_{\mathrm{QCD}} \\[3mm] \dfrac{m_\pi f_\pi}{f_a} \sqrt{\dfrac{z}{1-z^2}} , & T_{\mathrm{QCD}} < T \leq \dfrac{T_{\mathrm{QCD}}}{\gamma} \\[3mm] \dfrac{m_\pi f_\pi}{f_a} \sqrt{\dfrac{z}{1-z^2}} \left(\dfrac{\gamma T}{T_{\mathrm{QCD}}}\right)^{-b} , & T > \dfrac{T_{\mathrm{QCD}}}{\gamma} \end{cases} \tag{2.9}$$

where $\gamma \in (0,1)$ is a temperature parameter. The first and second terms in eq. (2.9) can also be defined as $m_{a,0}$ and $m_{a,\pi}$, respectively. In figure 1, we show the $Z_{\mathcal{N}}$ axion mass $m_a(T)$ as functions of the temperature T. The different colored lines correspond to the different values of $\mathcal{N}$, which are degenerated into the red line at the temperature $T \geq T_{\mathrm{QCD}}$. Compared with the canonical QCD axion [eq. (2.2)], we have a relation between their zero-temperature axion masses

$$\frac{m_{a,0}}{m_{a,0}^{\mathrm{QCD}}} = \frac{1}{\sqrt[4]{\pi}} \sqrt[4]{\frac{(1-z)(1+z)^3}{z^2}} \mathcal{N}^{3/4} z^{\mathcal{N}/2} , \tag{2.10}$$

which is suddenly exponentially suppressed at T_{QCD} due to the $Z_{\mathcal{N}}$ symmetry. The $Z_{\mathcal{N}}$ axion can also account for the DM through the trapped+kinetic misalignment mechanism, see refs. [26, 27] for more details.

3 Extended QCD axion mass mixing

In this section, we extend the QCD axion mass mixing and investigate the temperature effects in the mixing.

3.1 The model

For our purpose, we consider a minimal multiple QCD axions model, two $Z_{\mathcal{N}}$ axions ϕ_i ($i = 1, 2$), with the low-energy effective Lagrangian

$$
\mathcal{L} \supset \frac{1}{2} \sum_{i=1,2} \partial_\mu \phi_i \partial^\mu \phi_i - \frac{m_1^2(T) f_1^2}{\mathcal{N}_1^2} \left[1 - \cos\left(\mathcal{N}_1 \frac{\phi_1}{f_1} \right) \right]
$$
$$
- \frac{m_2^2(T) f_2^2}{\mathcal{N}_2^2} \left[1 - \cos\left(\mathcal{N}_1 \frac{\phi_1}{f_1} + \mathcal{N}_2 \frac{\phi_2}{f_2} \right) \right],
\tag{3.1}
$$

where $m_i(T)$ is the temperature-dependent axion mass corresponding to ϕ_i, and f_i is the axion decay constant. Here the axion mass $m_i(T)$ can be described by

$$
m_i(T) = \begin{cases}
\dfrac{m_\pi f_\pi}{\sqrt[4]{\pi} f_i} \sqrt[4]{\dfrac{1-z}{1+z}} \mathcal{N}_i^{3/4} z^{\mathcal{N}_i/2}, & T \leq T_{\mathrm{QCD}} \\[2ex]
\dfrac{m_\pi f_\pi}{f_i} \sqrt{\dfrac{z}{1-z^2}}, & T_{\mathrm{QCD}} < T \leq \dfrac{T_{\mathrm{QCD}}}{\gamma_i} \\[2ex]
\dfrac{m_\pi f_\pi}{f_i} \sqrt{\dfrac{z}{1-z^2}} \left(\dfrac{\gamma_i T}{T_{\mathrm{QCD}}} \right)^{-b}, & T > \dfrac{T_{\mathrm{QCD}}}{\gamma_i}
\end{cases}
\tag{3.2}
$$

where $\gamma_i \in (0, 1)$ is the temperature parameter, and we focus our attention on a case that[1]

$$
\frac{T_{\mathrm{QCD}}}{\gamma_1} > \frac{T_{\mathrm{QCD}}}{\gamma_2} \implies \gamma_1 < \gamma_2.
\tag{3.3}
$$

The first term in Eq. (3.2) corresponds to the zero-temperature axion mass

$$
m_{i,0} = \frac{m_\pi f_\pi}{\sqrt[4]{\pi} f_i} \sqrt[4]{\frac{1-z}{1+z}} \mathcal{N}_i^{3/4} z^{\mathcal{N}_i/2},
\tag{3.4}
$$

which is exponentially suppressed due to the $Z_{\mathcal{N}}$ symmetry. The second term in Eq. (3.2) corresponds to the mass

$$
m_{i,\pi} = \frac{m_\pi f_\pi}{f_i} \sqrt{\frac{z}{1-z^2}}.
\tag{3.5}
$$

It is necessary to first illustrate the distribution of axion mass m_i in the no mixing case, see figure 2. We choose two typical distributions for m_1 and m_2 with the red and blue lines, respectively. See table 1 for the model parameters.

---

[1] Notice that one can also assume $\gamma_1 > \gamma_2$, which will not affect our main results.
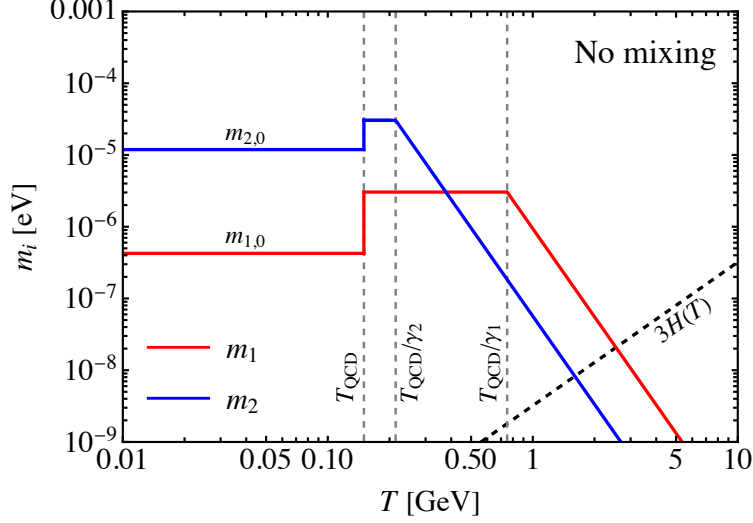
Figure 2. The illustration of the no mixing case. The red and blue solid lines represent the temperature-dependent axion masses $m_1(T)$ and $m_2(T)$, respectively. The three vertical gray lines represent the temperatures T_{QCD}, $T_{\mathrm{QCD}}/\gamma_2$, and $T_{\mathrm{QCD}}/\gamma_1$, respectively. The black dashed line represents the Hubble parameter $H(T)$. Notice that we have assumed $\gamma_1 < \gamma_2$. The model parameters can be found in table 1.

Then plugging the whole mixing potential of eq. (3.1) into the EOM

$$\ddot{\phi}_i + 3H\dot{\phi}_i + \frac{\partial V_{\mathrm{mix}}(\phi_i)}{\partial \phi_i} = 0 \,, \tag{3.6}$$

we derive the EOM of ϕ_i

$$\ddot{\phi}_2 + 3H\dot{\phi}_2 + \frac{m_2^2(T)f_2}{\mathcal{N}_2} \sin\left(\mathcal{N}_1\frac{\phi_1}{f_1} + \mathcal{N}_2\frac{\phi_2}{f_2}\right) = 0 \,, \tag{3.7}$$

$$\ddot{\phi}_1 + 3H\dot{\phi}_1 + \frac{m_1^2(T)f_1}{\mathcal{N}_1} \sin\left(\mathcal{N}_1\frac{\phi_1}{f_1}\right) + \frac{\mathcal{N}_1 m_2^2(T)f_2^2}{\mathcal{N}_2^2 f_1} \sin\left(\mathcal{N}_1\frac{\phi_1}{f_1} + \mathcal{N}_2\frac{\phi_2}{f_2}\right) = 0 \,, \quad (3.8)$$

where one dot represents a derivative with respect to the physical time t, two dots represent two derivatives with respect to the time, $\partial_{\phi_i} V_{\mathrm{mix}}$ represents the derivative of V_{mix} with respect to ϕ_i, and $H(T)$ is the Hubble parameter. If considering the oscillation amplitudes of ϕ_i are much smaller than the corresponding decay constants f_i, we can obtain the mass mixing matrix in our model

$$\mathbf{M}^2 = \begin{pmatrix} m_2^2(T) & \dfrac{\mathcal{N}_1 m_2^2(T)f_2}{\mathcal{N}_2 f_1} \\ \dfrac{\mathcal{N}_1 m_2^2(T)f_2}{\mathcal{N}_2 f_1} & m_1^2(T) + \dfrac{\mathcal{N}_1^2 m_2^2(T)f_2^2}{\mathcal{N}_2^2 f_1^2} \end{pmatrix} \,. \tag{3.9}$$

Diagonalizing the mass mixing matrix, we derive the heavy and light mass eigenstates a_h and a_l, respectively,

$$\begin{pmatrix} a_l \\ a_h \end{pmatrix} = \begin{pmatrix} \cos\alpha & \sin\alpha \\ -\sin\alpha & \cos\alpha \end{pmatrix} \begin{pmatrix} \phi_2 \\ \phi_1 \end{pmatrix} \,, \tag{3.10}$$

Scenarios	f_1 (GeV)	γ_1	$\mathcal{N}_1$	f_2 (GeV)	γ_2	$\mathcal{N}_2$	$T_\times$ (MeV)
No mixing	$10^{12.5}$	0.2	9	$10^{11.5}$	0.7	5	—
Mixing I	$10^{12.5}$	0.2	9	$10^{11.5}$	0.7	5	381.28
Mixing II	$10^{12.5}$	0.2	9	$10^{11.5}$	0.7	13	377.45
Mixing III	$10^{12.5}$	0.2	9	$10^{11.5}$	0.7	21	377.04

Table 1. The typical model parameters for f_i, γ_i, and $\mathcal{N}_i$ used in this work. In order to make clear comparisons, we try to minimize alteration to the model parameters and keep other parameters unchanged. Therefore, in the simplest case, we only need to fine-tune $\mathcal{N}_2$ to achieve our illustrative purpose. Here we also show the values of $T_\times$ in the mixing scenarios.

with the mass mixing angle α

$$\cos^2 \alpha(T) = \frac{1}{2} \left(1 + \frac{m_1^2(T) - m_2^2(T) + \dfrac{\mathcal{N}_1^2 m_2^2(T) f_2^2}{\mathcal{N}_2^2 f_1^2}}{m_h^2(T) - m_l^2(T)} \right), \tag{3.11}$$

where $m_h(T)$ and $m_l(T)$ (assuming $m_h > m_l$) are the corresponding mass eigenvalues

$$\begin{aligned} m_{h,l}^2(T) = &\frac{1}{2} \left[m_1^2(T) + m_2^2(T) + \frac{\mathcal{N}_1^2 m_2^2(T) f_2^2}{\mathcal{N}_2^2 f_1^2} \right] \\ &\pm \frac{1}{2\mathcal{N}_2^2 f_1^2} \left[-4\mathcal{N}_2^4 m_1^2(T) m_2^2(T) f_1^4 \right. \\ &\left. + \left(\mathcal{N}_1^2 m_2^2(T) f_2^2 + \mathcal{N}_2^2 f_1^2 \left(m_1^2(T) + m_2^2(T) \right) \right)^2 \right]^{1/2}. \end{aligned} \tag{3.12}$$

3.2 Level crossing in the mass mixing

In this subsection, we investigate the level crossing in the above extended QCD axion mass mixing. Since we have set $\gamma_1 < \gamma_2$ before, the following results and discussions are based on this assumption.

3.2.1 The mixing I

We first consider a mixing scenario that the zero-temperature axion mass $m_{2,0}$ of ϕ_2 is larger than the mass $m_{1,\pi}$ of ϕ_1

$$\frac{m_\pi f_\pi}{\sqrt[4]{\pi} f_2} \sqrt[4]{\frac{1-z}{1+z}} \mathcal{N}_2^{3/4} z^{\mathcal{N}_2/2} > \frac{m_\pi f_\pi}{f_1} \sqrt{\frac{z}{1-z^2}}, \tag{3.13}$$

then we have

$$\frac{f_2}{f_1} < \frac{1}{\sqrt[4]{\pi}} \sqrt[4]{\frac{(1+z)(1-z)^3}{z^2}} \mathcal{N}_2^{3/4} z^{\mathcal{N}_2/2} \simeq 0.73 \times 0.48^{\mathcal{N}_2/2} \mathcal{N}_2^{3/4}. \tag{3.14}$$

See figure 3 for the illustration of this mixing scenario. The red and blue lines correspond to the temperature-dependent mass eigenvalues $m_h(T)$ and $m_l(T)$ as functions of the cosmic
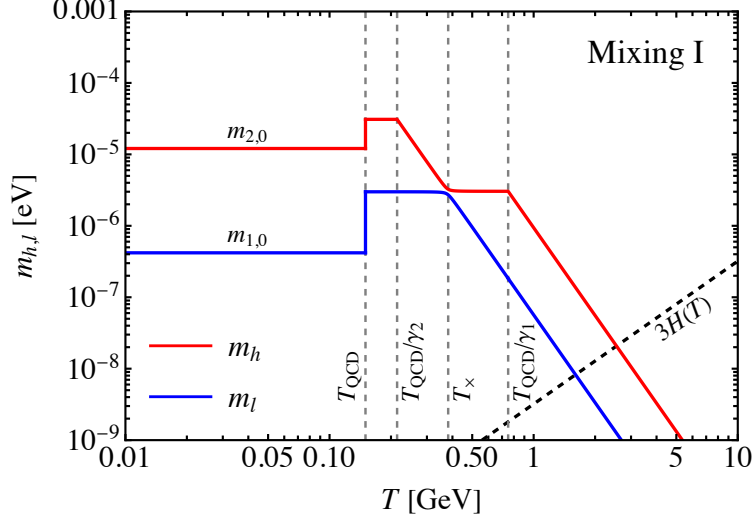
Figure 3. The illustration of the mixing I. The red and blue solid lines represent the temperature-dependent mass eigenvalues $m_h(T)$ and $m_l(T)$, respectively. The third vertical gray line represents the level crossing temperature $T_\times$. The model parameters can be found in table 1.

temperature T, respectively. To compare with the no mixing situation, here we use the same model parameters as in figure 2.

In this case, the level crossing can take place when the difference of $m_h^2(T) - m_l^2(T)$ gets a minimum value. By solving

$$\frac{d\left(m_h^2(T) - m_l^2(T)\right)}{dT} = 0\,, \tag{3.15}$$

we have the level crossing temperature in the mixing

$$T_\times = \frac{T_{\text{QCD}}}{\gamma_2}\left(\frac{\left(\mathcal{N}_1^2 f_2^2 + \mathcal{N}_2^2 f_1^2\right)^2}{\mathcal{N}_2^4 f_1^2 f_2^2 - \mathcal{N}_1^2 \mathcal{N}_2^2 f_2^4}\right)^{\frac{1}{2b}}\,, \tag{3.16}$$

which will last for a parametric duration

$$\Delta T_\times = \left|\frac{1}{\cos\alpha(T)}\frac{d\cos\alpha(T)}{dT}\right|^{-1}_{T=T_\times}\,, \tag{3.17}$$

corresponding to the time $\Delta t_\times$. Notice also that from eq. (3.16) we can obtain the following relation

$$\mathcal{N}_2^4 f_1^2 f_2^2 - \mathcal{N}_1^2 \mathcal{N}_2^2 f_2^4 > 0 \implies \frac{f_2}{f_1} < \frac{\mathcal{N}_2}{\mathcal{N}_1}\,. \tag{3.18}$$

Since we have assumed $\gamma_1 < \gamma_2$, the level crossing temperature $T_\times$ is not related to γ_1. See figure 3 with the third vertical gray line $T_\times \simeq 381.28\,\text{MeV}$. Here we discuss the temperature-dependent behavior of the axions in the mixing. At high temperatures, the heavy mass eigenstate a_h comprises the axion ϕ_1, while the light mass eigenstate a_l comprises the ϕ_2. With the cosmic temperature decreasing, the masse eigenvalues $m_h(T)$ and
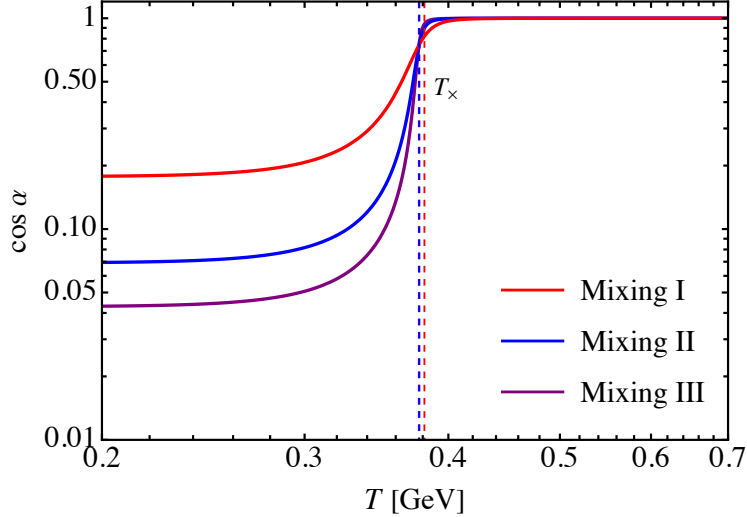
Figure 4. The mass mixing angle $\cos\alpha$ as functions of the cosmic temperature T. The red, blue, and purple solid lines correspond to the mixing I, II, and III, respectively. The vertical lines represent the corresponding level crossing temperatures $T_\times$.

$m_l(T)$ will approach to each other at $T_\times$ and then move away from each other. This asymptotic behavior is called the level crossing. After that, the a_h comprises the ϕ_2, and the a_l comprises the ϕ_1. The level crossing can lead to the adiabatic energy density transition between the ϕ_1 and ϕ_2. We also show the mass mixing angle $\cos\alpha$ in figure 4 with the red solid line. At high temperatures, the mixing angle is constant with $\cos\alpha = 1$ ($\alpha = 0$) until the level crossing occurs at $T_\times$, then it drops rapidly and stabilizes at a small value.

3.2.2 The mixing II

Based on the mixing I, it is natural to consider a situation where $\mathcal{N}_2$ is large enough, so that $m_{2,0}$ is smaller than $m_{1,\pi}$. Therefore, here we consider another scenario that the zero-temperature axion mass $m_{2,0}$ of ϕ_2 is smaller than the mass $m_{1,\pi}$ of ϕ_1, but larger than the zero-temperature axion mass $m_{1,0}$ of ϕ_1

$$\frac{m_\pi f_\pi}{\sqrt[4]{\pi} f_1}\sqrt[4]{\frac{1-z}{1+z}}\mathcal{N}_1^{3/4}z^{\mathcal{N}_1/2} < \frac{m_\pi f_\pi}{\sqrt[4]{\pi} f_2}\sqrt[4]{\frac{1-z}{1+z}}\mathcal{N}_2^{3/4}z^{\mathcal{N}_2/2} < \frac{m_\pi f_\pi}{f_1}\sqrt{\frac{z}{1-z^2}}, \quad (3.19)$$

then we have

$$0.73 \times 0.48^{\mathcal{N}_2/2}\mathcal{N}_2^{3/4} < \frac{f_2}{f_1} < 0.48^{(\mathcal{N}_2-\mathcal{N}_1)/2}\left(\frac{\mathcal{N}_2}{\mathcal{N}_1}\right)^{3/4}. \quad (3.20)$$

Notice that there is an additional relation that should be saturated first[2], the mass $m_{1,\pi}$ of ϕ_1 should be smaller than the mass $m_{2,\pi}$ of ϕ_2

$$\frac{m_\pi f_\pi}{f_1}\sqrt{\frac{z}{1-z^2}} < \frac{m_\pi f_\pi}{f_2}\sqrt{\frac{z}{1-z^2}} \implies \frac{f_2}{f_1} < 1. \quad (3.21)$$

---

[2]This relation can be naturally saturated in the mixing I since in that scenario the zero-temperature axion mass $m_{2,0}$ of ϕ_2 is larger than the mass $m_{1,\pi}$ of ϕ_1.
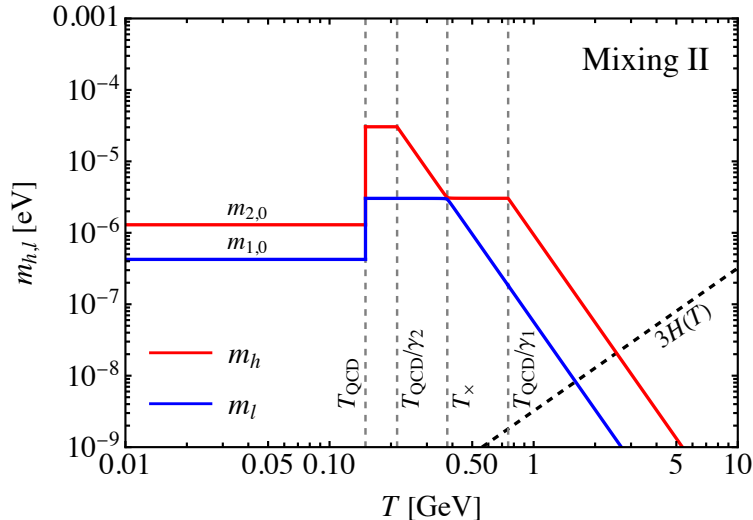
Figure 5. Same as figure 3 but for the mixing II.

See also figure 5 for the illustration of this mixing scenario. The model parameters can be found in table 1. The axion evolution in this scenario is basically similar to the mixing I, but at T_{QCD} it has a minor non-essential difference. Notice that the axion evolution at T_{QCD} is not the double level crossings case proposed in ref. [34], here the level crossing only occurs at $T_\times$. We also show in figure 4 the mass mixing angle $\cos\alpha$ in this case. Compared with the mixing I, the mixing angle will change more dramatically and eventually stabilize at a smaller value of $\cos\alpha$.

In fact, there is no fundamental distinction between the mixing I and II, and their axion evolution is similar. Nonetheless, in order to compare with another scenario discussed below, we feel that it is still necessary to list this scenario separately here.

3.2.3 The mixing III

Then we further consider the third mixing scenario that the zero-temperature axion mass $m_{2,0}$ of ϕ_2 is smaller than the zero-temperature axion mass $m_{1,0}$ of ϕ_1

$$\frac{f_2}{f_1} > 0.48^{(\mathcal{N}_2 - \mathcal{N}_1)/2} \left(\frac{\mathcal{N}_2}{\mathcal{N}_1}\right)^{3/4}. \tag{3.22}$$

Notice that eq. (3.21) should also be saturated here. We show in figure 6 the illustration of this mixing scenario. The model parameters are also listed in table 1.

Comparing figures 5 with 6, we find that they appear similar, but in fact they have fundamental differences. It is necessary to clarify the axion evolution in this scenario. At high temperatures, the heavy mass eigenstate a_h comprises the axion ϕ_1, while the light mass eigenstate a_l comprises the ϕ_2. With the cosmic temperature decreasing, the first level crossing occurs at $T_\times$, the masse eigenvalues $m_h(T)$ and $m_l(T)$ will approach to each other and then move away from each other. After that, the a_h comprises the ϕ_2 and the a_l comprises the ϕ_1 until T_{QCD}. So far, the axion evolution is the same as the above scenarios
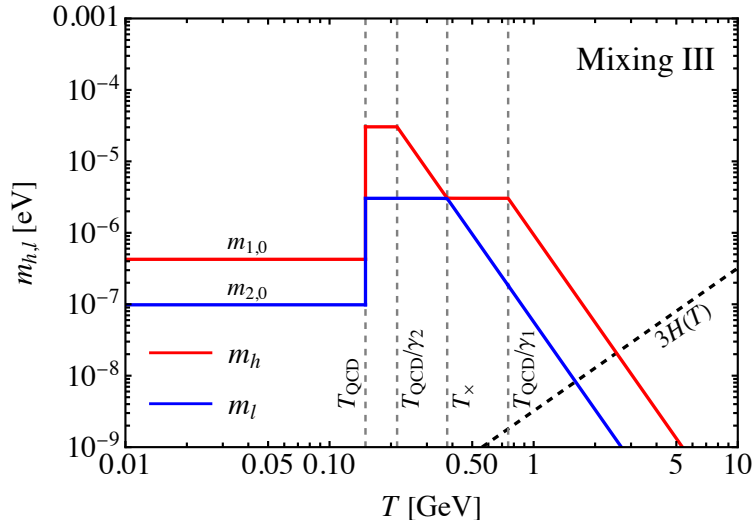
Figure 6. Same as figure 3 but for the mixing III. Notice that the first and second level crossings can take place at $T_\times$ and T_{QCD}, respectively.

mixing I and II. However, this will change at the temperature T_{QCD}. The second level crossing will take place at T_{QCD}, then the heavy a_h will comprise the ϕ_1 and the light one a_l will comprise the ϕ_2 again. This behavior is called the double level crossings, which is also the main difference between the mixing II and III. The transition of axion energy density in this scenario will also be drastically altered. The mass mixing angle $\cos\alpha$ in this scenario can be found in figure 4 with the purple line.

We close this subsection by discussing the conditions for above three mixing scenarios to occur. For comparison, we plot them in the $\{\mathcal{N}_2,\ f_2/f_1\}$ plane, see figure 7 with the shadow regions. The red, blue, and purple shadow regions correspond to the mixing I, II, and III, respectively. The red line is given by eq. (3.18), the blue line is given by eq. (3.14), the purple line is given by eq. (3.20), and the gray solid line is given by eq. (3.21), respectively. Notice that the vertical gray line represents $\mathcal{N}_2 = \mathcal{N}_1 = 9$. The parameter $\mathcal{N}_1$ will affect the conditions for all three mixing scenarios, which can be seen as shifting this vertical line laterally to different values of $\mathcal{N}_1$ in the plot.

3.3 Transition of axion energy density

In this subsection, we briefly discuss the energy density transition between the two axions in our mixing scenarios.

In the mass mixing, the adiabatic transition can take place if both the comoving axion numbers of the eigenstates a_h and a_l are separately conserved at the level crossing temperature [39, 53]. The condition for adiabatic transition can be described by

$$\Delta t_\times \gg \max\left[\left.\frac{2\pi}{m_l(T)}\right|_{T=T_\times},\ \left.\frac{2\pi}{m_h(T)-m_l(T)}\right|_{T=T_\times}\right], \tag{3.23}$$

corresponding to the temperature in eq. (3.17). One can also numerically check this inequality to determine whether the adiabatic condition is met at $T_\times$.
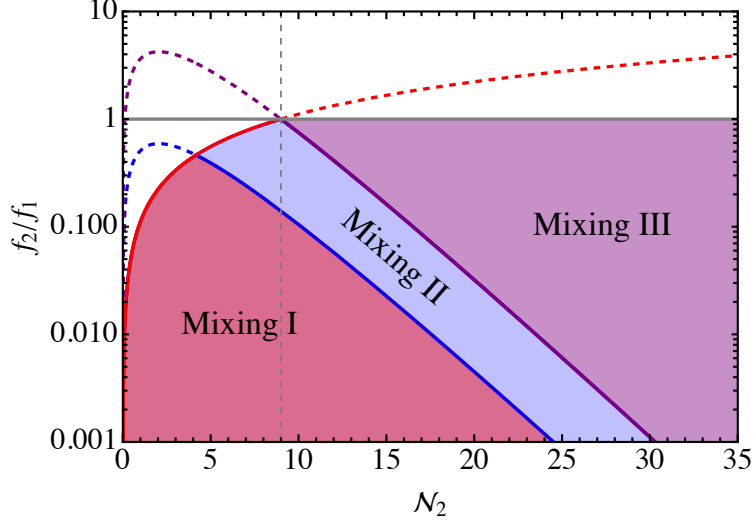
Figure 7. The conditions for the mixing I, II, and III to occur in the $\{\mathcal{N}_2, f_2/f_1\}$ plane. The red, blue, and purple shadow regions correspond to the mixing I, II, and III, respectively. The gray solid line represents $f_2/f_1 = 1$. The vertical gray line represents $\mathcal{N}_2 = 9$. Here we set $\mathcal{N}_1 = 9$. Note also that $\mathcal{N}_1, \mathcal{N}_2 = 2k + 1, k \in \mathbb{N}^+$.

Here we only illustrate how the axion energy density is transferred in the mixing, without intending to discuss the further details. Since the axion evolution in the mixing I and II is similar, their energy density transitions are similar as well. Hence, we will only discuss the mixing II. In this scenario, at high temperatures the axion fields ϕ_1 and ϕ_2 are frozen at the arbitrary initial misalignment angles, and start to oscillate at the corresponding oscillation temperatures T_{osc}. Then during the period from T_{osc} to $T_\times$, the axion energy density is adiabatic invariant with a comoving number. If the condition for adiabatic transition is saturated at $T_\times$, the energy density of ϕ_1 will be transferred to ϕ_2 and vice versa. Then the final axion energy density can be further calculated through the trapped+kinetic misalignment mechanism.

In the mixing III, the axion energy transition before the QCD phase transition critical temperature T_{QCD} is similar to that discussed above, but it begins to diverge at T_{QCD}. Since the second level crossing can occur at T_{QCD}, then the a_h will comprise the ϕ_1 and the a_l will comprise the ϕ_2 again, so the final axion energy density will differ based on the corresponding zero-temperature axion masses. Notice that the axion energy density at the second level crossing is non-adiabatic.

4   Conclusion

In summary, we have extended the QCD axion mass mixing in the early Universe and investigated the temperature effects in the mixing. We first review the canonical QCD axion and the lighter $Z_\mathcal{N}$ QCD axion. Then we extend the QCD axion mass mixing and investigate the temperature effects. Finally, we briefly discuss the energy density transition between the two axions in the mixing.

For our purpose, we consider the mass mixing between two $Z_\mathcal{N}$ axions during the QCD phase transition, resulting in three mixing scenarios, the mixing I, II, and III. This can be accomplished by fine-tuning the model parameters, such as the axion decay constants f_i, the temperature parameters γ_i, and also the number of $\mathcal{N}_i$. The level crossing in these three mixing scenarios and the conditions for them to occur in the $\{\mathcal{N}_2,\, f_2/f_1\}$ plane are studied and illustrated in detail.

In the mixing I and II, the level crossing can take place before the QCD phase transition critical temperature T_{QCD}, while the cosmological evolution of the mass eigenvalues at T_{QCD} has a minor non-essential difference. In order to compare with the mixing III, we list the mixing II separately. In the mixing III, we find that the double level crossings can take place before and at T_{QCD}, respectively. Although the axion evolution in the mixing II and III appears similar, they have fundamental differences. In the mixing II (or I), the axion evolution from high temperatures to low temperatures can be approximately described by $\phi_1 \to \phi_2$ and $\phi_2 \to \phi_1$, while in the mixing III this is described by $\phi_1 \to \phi_2 \to \phi_1$ and $\phi_2 \to \phi_1 \to \phi_2$. Therefore, the final axion energy density will differ based on the corresponding zero-temperature axion masses.

Beyond its potential role as cold DM, the extended QCD axion mass mixing framework presented in our scenarios may also yield other intriguing cosmological implications, warranting further investigation.

Acknowledgments

References

[1] R. Peccei and H. R. Quinn, *CP Conservation in the Presence of Instantons*, *Phys. Rev. Lett.* **38** (1977) 1440–1443.

[2] R. Peccei and H. R. Quinn, *Constraints Imposed by CP Conservation in the Presence of Instantons*, *Phys. Rev. D* **16** (1977) 1791–1797.

[3] S. Weinberg, *A New Light Boson?*, *Phys. Rev. Lett.* **40** (1978) 223–226.

[4] F. Wilczek, *Problem of Strong P and T Invariance in the Presence of Instantons*, *Phys. Rev. Lett.* **40** (1978) 279–282.

[5] J. E. Kim, *Weak Interaction Singlet and Strong CP Invariance*, *Phys. Rev. Lett.* **43** (1979) 103.

[6] M. A. Shifman, A. I. Vainshtein and V. I. Zakharov, *Can Confinement Ensure Natural CP Invariance of Strong Interactions?*, *Nucl. Phys. B* **166** (1980) 493–506.

[7] M. Dine, W. Fischler and M. Srednicki, *A Simple Solution to the Strong CP Problem with a Harmless Axion*, *Phys. Lett. B* **104** (1981) 199–202.

[8] A. R. Zhitnitsky, *On Possible Suppression of the Axion Hadron Interactions. (In Russian)*, *Sov. J. Nucl. Phys.* **31** (1980) 260.

[9] G. 't Hooft, *Symmetry Breaking Through Bell-Jackiw Anomalies*, *Phys. Rev. Lett.* **37** (1976) 8–11.

[10] G. 't Hooft, *Computation of the Quantum Effects Due to a Four-Dimensional Pseudoparticle*, *Phys. Rev. D* **14** (1976) 3432–3450.

[11] A. Hook, *TASI Lectures on the Strong CP Problem and Axions*, PoS **TASI2018** (2019) 004, [1812.02669].

[12] J. Preskill, M. B. Wise and F. Wilczek, *Cosmology of the Invisible Axion*, *Phys. Lett. B* **120** (1983) 127–132.

[13] L. Abbott and P. Sikivie, *A Cosmological Bound on the Invisible Axion*, *Phys. Lett. B* **120** (1983) 133–136.

[14] M. Dine and W. Fischler, *The Not So Harmless Axion*, *Phys. Lett. B* **120** (1983) 137–141.

[15] D. J. E. Marsh, *Axion Cosmology*, *Phys. Rept.* **643** (2016) 1–79, [1510.07633].

[16] L. Di Luzio, M. Giannotti, E. Nardi and L. Visinelli, *The landscape of QCD axion models*, *Phys. Rept.* **870** (2020) 1–117, [2003.01100].

[17] C. A. J. O'Hare, *Cosmology of axion dark matter*, *PoS* **COSMICWISPers** (2024) 040, [2403.17697].

[18] G. Raffelt and D. Seckel, *Bounds on Exotic Particle Interactions from SN 1987a*, *Phys. Rev. Lett.* **60** (1988) 1793.

[19] M. S. Turner, *Axions from SN 1987a*, *Phys. Rev. Lett.* **60** (1988) 1797.

[20] R. Mayle, J. R. Wilson, J. R. Ellis, K. A. Olive, D. N. Schramm and G. Steigman, *Constraints on Axions from SN 1987a*, *Phys. Lett. B* **203** (1988) 188–196.

[21] L. B. Leinson, *Axion mass limit from observations of the neutron star in Cassiopeia A*, *JCAP* **08** (2014) 031, [1405.6873].

[22] K. Hamaguchi, N. Nagata, K. Yanagi and J. Zheng, *Limit on the Axion Decay Constant from the Cooling Neutron Star in Cassiopeia A*, *Phys. Rev. D* **98** (2018) 103015, [1806.07151].

[23] M. Buschmann, C. Dessert, J. W. Foster, A. J. Long and B. R. Safdi, *Upper Limit on the QCD Axion Mass from Isolated Neutron Star Cooling*, *Phys. Rev. Lett.* **128** (2022) 091102, [2111.09892].

[24] A. Hook, *Solving the Hierarchy Problem Discretely*, *Phys. Rev. Lett.* **120** (2018) 261802, [1802.10093].

[25] L. Di Luzio, B. Gavela, P. Quilez and A. Ringwald, *An even lighter QCD axion*, *JHEP* **05** (2021) 184, [2102.00012].

[26] L. Di Luzio, B. Gavela, P. Quilez and A. Ringwald, *Dark matter from an even lighter QCD axion: trapped misalignment*, *JCAP* **10** (2021) 001, [2102.01082].

[27] R. T. Co, L. J. Hall and K. Harigaya, *Axion Kinetic Misalignment Mechanism*, *Phys. Rev. Lett.* **124** (2020) 251802, [1910.14152].

[28] A. Arvanitaki, S. Dimopoulos, S. Dubovsky, N. Kaloper and J. March-Russell, *String Axiverse*, *Phys. Rev. D* **81** (2010) 123530, [0905.4720].

[29] M. Cicoli, M. Goodsell and A. Ringwald, *The type IIB string axiverse and its low-energy phenomenology*, *JHEP* **10** (2012) 146, [1206.0819].

[30] M. Demirtas, N. Gendler, C. Long, L. McAllister and J. Moritz, *PQ axiverse*, *JHEP* **06** (2023) 092, [2112.04503].

[31] C. T. Hill and G. G. Ross, *Models and New Phenomenological Implications of a Class of Pseudogoldstone Bosons*, *Nucl. Phys. B* **311** (1988) 253–297.

[32] R. Daido, N. Kitajima and F. Takahashi, *Level crossing between the QCD axion and an axionlike particle*, *Phys. Rev. D* **93** (2016) 075027, [1510.06675].

[33] D. Cyncynates and J. O. Thompson, *Heavy QCD axion dark matter from avoided level crossing*, *Phys. Rev. D* **108** (2023) L091703, [2306.04678].

[34] H.-J. Li, Y.-Q. Peng, W. Chao and Y.-F. Zhou, *Light QCD axion dark matter from double level crossings*, *Phys. Lett. B* **849** (2024) 138444, [2310.02126].

[35] L. Wolfenstein, *Neutrino Oscillations in Matter*, *Phys. Rev. D* **17** (1978) 2369–2374.

[36] S. P. Mikheyev and A. Y. Smirnov, *Resonance Amplification of Oscillations in Matter and Spectroscopy of Solar Neutrinos*, *Sov. J. Nucl. Phys.* **42** (1985) 913–917.

[37] S. P. Mikheev and A. Y. Smirnov, *Resonant amplification of neutrino oscillations in matter and solar neutrino spectroscopy*, *Nuovo Cim. C* **9** (1986) 17–26.

[38] N. Kitajima and F. Takahashi, *Resonant conversions of QCD axions into hidden axions and suppressed isocurvature perturbations*, *JCAP* **01** (2015) 032, [1411.2011].

[39] S.-Y. Ho, K. Saikawa and F. Takahashi, *Enhanced photon coupling of ALP dark matter adiabatically converted from the QCD axion*, *JCAP* **10** (2018) 042, [1806.09551].

[40] D. Cyncynates, T. Giurgica-Tiron, O. Simon and J. O. Thompson, *Resonant nonlinear pairs in the axiverse and their late-time direct and astrophysical signatures*, *Phys. Rev. D* **105** (2022) 055005, [2109.09755].

[41] H.-J. Li, *Axion dark matter with explicit Peccei-Quinn symmetry breaking in the axiverse*, *JCAP* **09** (2024) 025, [2307.09245].

[42] R. Daido, N. Kitajima and F. Takahashi, *Domain Wall Formation from Level Crossing in the Axiverse*, *Phys. Rev. D* **92** (2015) 063512, [1505.07670].

[43] D. Cyncynates, O. Simon, J. O. Thompson and Z. J. Weiner, *Nonperturbative structure in coupled axion sectors and implications for direct detection*, *Phys. Rev. D* **106** (2022) 083503, [2208.05501].

[44] Z. Chen, A. Kobakhidze, C. A. J. O'Hare, Z. S. C. Picker and G. Pierobon, *Cosmology of the companion-axion model: dark matter, gravitational waves, and primordial black holes*, 2110.11014.

[45] H.-J. Li and Y.-F. Zhou, *Gravitational waves from axion domain walls in double level crossings*, 2401.09138.

[46] K. Müürsepp, E. Nardi and C. Smarra, *Can the QCD axion feed a dark energy component?*, 2405.00090.

[47] K. Müürsepp, *On the viability of the QCD axion - dark energy transition*, 5, 2024. 2405.20478.

[48] H.-J. Li and Y.-F. Zhou, *Mass mixing between QCD axions*, 2408.00267.

[49] S. Borsanyi et al., *Calculation of the axion mass based on high-temperature lattice quantum chromodynamics*, *Nature* **539** (2016) 69–71, [1606.07494].

[50] D. H. Lyth, *Axions and inflation: Sitting in the vacuum*, *Phys. Rev. D* **45** (1992) 3394–3404.

[51] L. Visinelli and P. Gondolo, *Dark Matter Axions Revisited*, *Phys. Rev. D* **80** (2009) 035024, [0903.4377].

[52] PLANCK collaboration, N. Aghanim et al., *Planck 2018 results. VI. Cosmological parameters*, *Astron. Astrophys.* **641** (2020) A6, [1807.06209]. [Erratum: Astron.Astrophys. 652, C4 (2021)].

[53] M. Devaud, V. Leroy, J.-C. Bacri and T. Hocquet, "The adiabatic invariant of any harmonic oscillator : an unexpected application of Glauber's formalism." working paper or preprint, Dec., 2007.